

Toward a Definitive Assessment of the Impact of Leaf Angle Distributions on LiDAR Structural Metrics

R. Wible¹, K. Patki¹, K. Krause², and J. van Aardt¹

¹Rochester Institute of Technology, Chester F. Carlson Center for Imaging Science, 54 Lomb Memorial Drive, Rochester, NY, 14623, USA
Email: vanaardt@cis.rit.edu

²Battelle, 1685 38th St. Suite 100, Boulder, CO, 80301, USA
Email: kkrause@battelleecology.org

1. Introduction

Ecological research relies on measurement and mapping of the changing patterns in biochemical and structural traits of vegetation regions over time, which enables ecologists to quantify and understand carbon cycling processes and its impact on global warming (Zhao et al., 2009). Such measurements are obtained using remote sensing, where established relationships between imaging spectroscopy and light detection and ranging (LiDAR) signals and plant functional traits like nutrient levels, leaf area index (LAI), leaf area angles, etc. already exist. However, little work exists on a definitive assessment of especially the linkages between spectral-structural variation.

Variation in radiometric and LiDAR signals can be attributed to many factors, such as leaf and wood optical properties, canopy attributes (LAI, leaf and stem orientation, and foliage clumping), background soil reflectance, illumination conditions, and viewing geometry, among others (Asner, 1998; Ollinger, 2011). Such properties can be directly or indirectly related to both the underlying biochemistry and the leaf structural properties (Ollinger, 2011; Baldocchi et al., 2020). For example, some of this variation can be mitigated by properly selecting temporal specifics for data collection, and via a better understanding of the impacts of structural variation and its impact on spectral response.

The overarching objective of this project therefore is to better understand the connection between plant (forest) structure and traits and thereby improve interpretation of remote sensing data in order to better map and monitor ecosystems assess. The specific objective is to assess the impact of forest leaf angle distribution (LAD) on both spectral and structural approaches to forest trait assessment. This was achieved by constructing a detailed, physics- and biophysics-based virtual scene.

2. Data and Methods

2.1 Research Site

The study area is a 500x700m tract located at the Prospect Hill tract within Harvard Forest, a National Ecological Observatory Network (NEON) NEON research site, located in Petersham, Massachusetts, USA (42°32'19.79"N, 72°10'31.81"W). The area consists of a mix of coniferous and deciduous trees, shrubs, and bushes, with prominent species Eastern Hemlock (*Tsuga canadensis*), Red Maple (*Acer rubrum*), Winter Berry (*Ilex verticillata*), Yellow Birch (*Betula alleghaniensis*), Northern Red Oak (*Quercus rubra*) and Mountain laurel (*Kalmia latifolia*).

2.2 Simulation Development

In order to understand the impact of changing leaf angle distribution, we built a virtual 3D model of a complex forest, with which we can experiment with leaf angles for each tree. We gathered field data from the online Harvard Forest Data Archive (harvardforest1.fas.harvard.edu), which contains information about geographic locations, height, and diameter at breast height (DBH) values of all plants.

3D models of vegetation were obtained from OnyxTREE BROADLEAF (V. 7.0) and OnyxTREE CONIFER (V. 7.0), a software suite used for procedural modeling of vegetation (www.onyxtree.com) The software requires a number of tree parameters as inputs and outputs faceted triangular meshes of the trees (Romanczyk et al., 2013). Multiple model variants for common species were created using OnyxTREE and instantiated in the scene at provided positions, so that the species at least matched the larger genus. Optical properties (reflectance and transmittance) for each species were obtained from real

measurements taken from the online ecological spectral database ECOSIS (ecosis.org). Spectral variation was created via PROSPECT (pypi.org/project/prosail), by randomly adjusting leaf parameters.

We used DIRSIG, a physics-based rendering and simulation tool designed and developed at RIT, for virtual image and LiDAR data generation. DIRSIG uses Monte Carlo ray tracing and is capable of capturing radiometrically accurate images of virtual scenes with passive illumination (sunlight, skylight, moonlight, starlight, and in-scene lights) in the Visible-NIR-SWIR wavelength ranges (Romanczyk et al., 2013). We obtained the images for this study using DIRSIG version 5 (2021.19). The spectral specifications used for the imager in DIRSIG were: i) wavelengths ranging from 400-1100nm (to spectral index derivation), ii) wavelength band centers separated by 5nm, iii) a FWHM bandwidth of 5nm, and iv) a Gaussian band shape; these parameters were based on the NEON Airborne Observation Platform (AOP) near-infrared imaging spectrometer specifications. Spatial specifications used were: i) pixel array of 1100 x 800 (virtual hyperspectral 2D spatial array to simplify data collection), ii) a pixel size of 22x22um, and iii) an imager placed at the center of the virtual scene at a height of 3km to capture the entire plot. The scenes were collected at 10h00 Eastern Standard Time (EST). The LiDAR simulation specifications were based on a Gemini ALTM LiDAR system (Table 1). Platform motion was modeled based on GPS/IMS data from the 2019 NEON platform and directly input into the DIRSIG platform motion file. Simulated data were compared to the 2019 NEON sensor data as three main categories: i) visual inspection, ii) spectral signatures/indices, and iii) LiDAR data, in terms of a limited statistical analysis of height and structure.

Table 1. LiDAR simulation specifications, as per the Gemini ALTM LiDAR system.

Wavelength	1064nm
Accuracies	5-30cm elevation; 1/ 5,500 x Altitude (m AGL) horizontal
Effective laser repetition rate	Programmable; 33-167kHz
Scan width (FOV)	Programmable; 0-50°
Scan frequency	Programmable; 0-70Hz
Beam divergence	Dual divergence: 0.25mrad (1/e) and 0.8 mrad (1/e)
Range/intensity capture	Up to four range/intensity measurements, including 1 st , 2 nd , 3 rd , and last returns

3. Results and Discussion

Simulated images from the RGB, imaging spectroscopy (HSI), and LiDAR sensors were successfully simulated (Figures 1a-c), for i) a 1024x512 RGB image (3,000 meters above sea level), ii) a 246 band HSI image (380-2500nm), and iii) a 40x30m LiDAR discrete point cloud. We observed that the variation in canopy color, tree species, and density are clearly visible, thus providing a realistic feel to the scene (Figure 1a). Visually the real image looks denser with a high percentage of trees overlapping, even though the simulation is geographically accurate. This discrepancy was attributed to OnyxTREE models not incorporating crown competition.

Spectrally the images were expected to be similar since the simulation used signatures from the real NEON HSI image. Figure 1b shows this to be mostly true, except for two classes in the simulated plot that exhibited almost twice as large values as the other vegetative signatures; this was attributed to the outer 100m buffer that surrounds the 3D model.

Structurally the 3D model heights and DBH values were based on field and sensor data, so the expectation was that the simulated values will mirror reality. The only simulated data initially available for analysis was a 40x30m discrete LiDAR point cloud (Figure 1c). Next steps will include incorporation of planophile and erectophile leaf distributions, and assessing their impact on especially discrete return LiDAR metrics (Figure 2 shows an initial spectral comparison).

4. Conclusions

The validation and extended LAD impact analysis of the 3D DIRSIG model is not complete. We presented an initial functionality, where we have developed a spectrally and structurally robust virtual scene of an actual forest site from Harvard Forest, USA. We have shown the capability to simulate both HSI and LiDAR sensors, as well as vary LAD. Next steps include a more extensive vetting of the actual scene, followed by an assessment of how field-observed LAD values, and the variation thereof, impact

both spectral and LiDAR metrics associated with forest trait assessment. Additional results for the structural analysis will be presented at the conference.

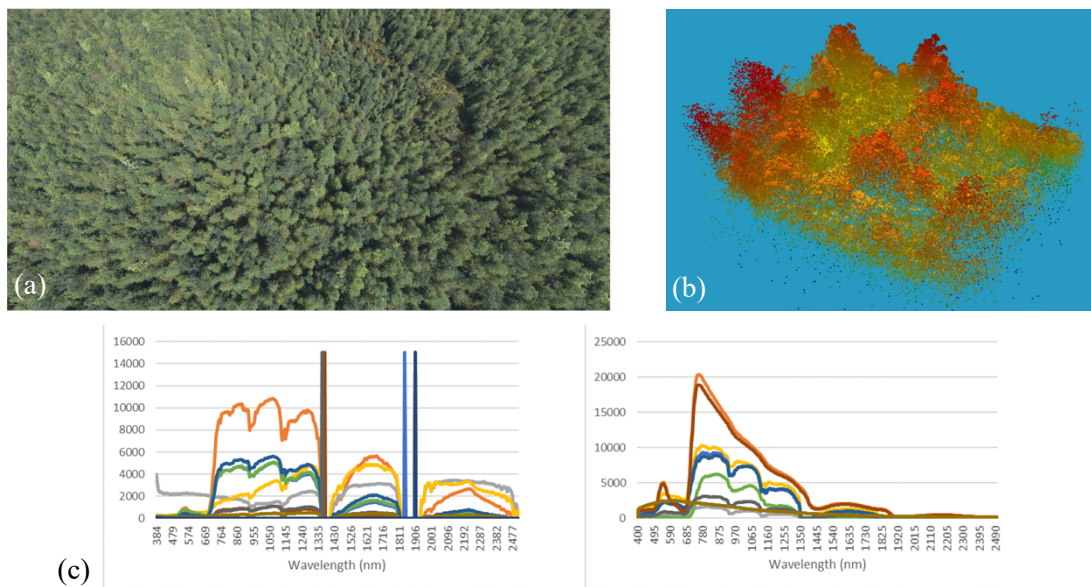


Figure 1: a) RGB rendering of the Harvard Forest Scene (1024x512 pixels); b) a comparison of spectral profiles (random species); and c) the simulated 40x30m discrete return LiDAR point cloud.

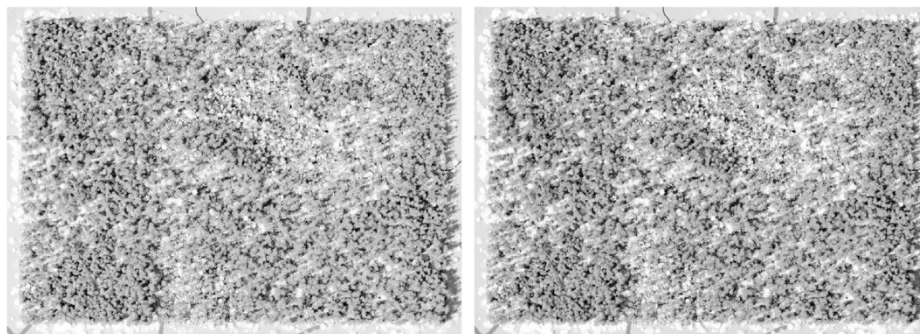


Figure 2: An initial, qualitative spectral comparison (500x700m) of planophile (left) vs. erectophile (right) LAD, as expressed via simplistic normalized difference vegetation index (NDVI) images (dark = low, bright = higher). Next steps will involve more explicit LAD definitions and an assessment of their impacts on both spectral and structural forest traits.

Acknowledgements

We gratefully acknowledge funding from the National Geospatial Intelligence Agency (award #HMO476010008) and NASA (award # 80NSSC20K1730/PO806052). Any findings and opinions expressed here are those of the authors alone.

References

- Asner GP, 1998, Biophysical and Biochemical Sources of Variability in Canopy Reflectance, *Remote Sensing of Environment* 64(3): 234-253.
- Baldocchi D, Y Ryu, B Dechant, E Eichelmann, K Hemes, S Ma, CR Sanchez, R Shortt, D Szutu, A Valach, J Verfaillie, G Badgley, Y Zeng, and JA Berry, 2020, Outgoing Near-Infrared Radiation From Vegetation Scales With Canopy Photosynthesis Across a Spectrum of Function, Structure, Physiological Capacity, and Weather, *Journal of Geophysical Research: Biogeosciences* 10.1029/2019JG005534 (17p).
- Ollinger S, 2011, Sources of variability in canopy reflectance and the convergent properties of plants, *New Phytologist* 189: 375-394.
- Romanczyk P, , 2013, Assessing the impact of broadleaf tree structure on airborne full-waveform small-footprint LiDAR signals through simulation, *Canadian Journal of Remote Sensing* 39(1): S60-S72.
- Zhao K, S Popescu, and R Nelson, 2009, Lidar remote sensing of forest biomass: A scale-invariant estimation approach using airborne lasers, *Remote Sensing of Environment* 113(1): 182-196.